Non-Rigid Image Registration using a Parameter-Free Elastic Model

Wladimir Peckar, Christoph Schnörr, Karl Rohr,
and H. Siegfried Stiehl

Universität Hamburg, FB Informatik, AB Kognitive Systeme,
Vogt-Kölln-Str. 30, D-22527 Hamburg, Germany
peckar@informatik.uni-hamburg.de

Abstract

The paper presents a new *parameter-free* approach to non-rigid image registration, where displacements, obtained through a mapping of boundary structures in the source and target image, are incorporated as hard constraints into elastic image deformation. As a consequence, our approach does not contain any parameters of the deformation model (elastic constants). The approach guarantees the *exact* correspondence of boundary structures after elastic transformation provided that correct input data are available. We describe a linear and an incremental model, the latter model allows to cope also with *large* deformations. Experimental results for 2-D and 3-D synthetic as well as real medical images are presented.

1 Introduction

Image registration aims at finding a transformation between different object representations. A typical application in medicine is, for example, the registration of human brain tomograms, where combination of data form different sources helps a physician to better locate and/or identify diagnostically or, respectively, therapeutically relevant structures in images. Formally, a mathematical transformation is applied, which puts one object representation (source image) into best possible spatial correspondence with another one (target image). Important criteria for assessing the performance of registration schemes are accuracy, robustness, and time required to compute the transformation.

The non-rigid registration approach, presented in this paper, belongs to the class of *physically-based numerical* methods (e.g., [1], [6], [9]), where non-rigid transformations are modeled as deformations of physical bodies (elastic solids, viscous fluids) driven by applied forces. The word "numerical" is used in the definition of this group of methods in order to avoid confusion with some other methods, e.g. thin-plate spline models [3], [16], which also have a physical motivation. Driving forces in physically-based numerical methods are usually derived from image data using some similarity measure and transformations are then computed by using finite difference or finite element discretizations of motion equations of the underlying materials.

In this paper, we propose a parameter-free registration model based on the non-linear equilibrium equations of elasticity theory. We carried out two different linearizations of

BMVC 1998 doi:10.5244/C.12.14

the equilibrium equations to obtain, correspondingly, our linear and incremental model. Both models can be applied for image registration tasks. Instead of forces, we used a set of hard constraints (in our case displacements) obtained by mapping boundary structures in the source image to those in the target image. The constraints are incorporated in addition to the conditions on the image boundary into the elastic deformation model. Discrete representations of both the linear and incremental model are based on the finite element method (FEM), which is advantageous compared to traditionally implemented finite differences, since it allows to cope with complicated boundary conditions.

The principal advantages of our approach as compared to standard physically-based numerical registration methods are: i) We do not use any local *intensity-based* similarity measure, since intensity properties alone are not always reliable features, e.g. in the case of non-rigid multi-modality registration. ii) Driving forces are *implicitly* used in our approach via incorporating prescribed displacements as constraints. As a consequence, the remaining parameters of the deformation model (elastic constants) drop out from the mathematical formulation of our registration approach; thus the model becomes completely *parameter-free*. iii) Since there exists a unique solution to the mathematical problem associated with our registration approach, it can always be guaranteed that the required deformation is obtained and that certain structures in the source image are *exactly* matched with those of the target image due to the constraints, provided that correct input data are available. iv) By using the incremental model, we obviate the known limitation of models based on linearized elasticity theory (see, for example, [1]), arising from the unrealistic assumption of small deformations.

Several other physically-based numerical approaches are known in the literature. Broit [5] originally used a model derived from elasticity theory to automatically find an optimal mapping between a CT image and an atlas of brain anatomy. This linear model assumed small deformations. The applied forces have been derived by correlating intensity-based properties in local regions in the source and target image. This model has been improved through the use of a multi-resolution scheme by Bajcsy and Kovačič [1] and later by Schormann et al. [17], to increase the speed of computations and to avoid local minima. A probabilistic model based on the FEM, which has been reported to have properties similar to those of [5], [1], has been proposed by Gee et al. [12].

Because of the potentially large variability of anatomical structures, possible deformations required to map a source onto a target image are not limited to locally small deformations. To cope with this problem, another approach in the class of physically-based numerical methods based on the theory of fluid mechanics has been introduced by Christensen et al. [6] (and later improved by Bro-Nielsen and Gramkow [4] to increase speed). A common drawback of this fluid model in comparison to the elastic approaches mentioned above is that a local intensity-based similarity measure is still used for the derivation of forces.

Davatzikos et al. [10] proposed a linear elastic model based on a boundary mapping, for which no local similarity measure is used. The elastic deformation is driven by external forces obtained from mapping parametric representations of the outer cortical surface and the boundary of the ventricles. This 2-D model has then been extended in [9] to 3-D in such a way that it can also cope with inhomogeneous deformations. Though this model is closely related to our approach, the principal differences are that i) it assumes only small deformations and ii) is parameter-dependent (the values of elastic constants have to be empirically determined to obtain optimal registration results).

2 Parameter-Free Registration Model

This section formally describes our elastic registration approach based upon two linearizations of the non-linear equilibrium equations of linearized elasticity. We use variational formulations of model equations, which allow us to straightforwardly obtain their discrete representations, as it will be shown later in this section.

2.1 Model Equations

Elastic registration can be interpreted as finding a state of static equilibrium of the source image, represented as an elastic body, under applied external forces.

Let Ω be a subset of $\mathcal{R}^3$ with a continuous boundary Γ. The non-linear equilibrium equation with the homogeneous Dirichlet boundary condition can be written as [8]:

$$\begin{cases} \mathbf{A}(\mathbf{u}) = \mathbf{f} \ \text{ in } \Omega, \\ \mathbf{u} = \mathbf{0} \ \text{ on } \Gamma, \end{cases} \tag{1}$$

where $\mathbf{A}(\mathbf{u})$ is the non-linear elasticity operator, $\mathbf{f}$ is a vector field of applied forces, and $\mathbf{u}$ denotes the unknown displacement field.

To obtain a first linearization of (1), which corresponds to our linear model, we compute the derivative of the non-linear elasticity operator at the origin and replace $\mathbf{A}(\mathbf{u})$ in (1) through $\mathbf{A}'(\mathbf{0})\mathbf{u}$ under the assumption of small displacements. The weak or variational formulation of the linearized equilibrium equation is then given as [8]: Find $\mathbf{u} \in \mathbf{V}$ such that

$$a(\mathbf{u}, \mathbf{v}) = f(\mathbf{v}), \quad \forall \mathbf{v} \in \mathbf{V} := \{\mathbf{v} \in (\mathcal{H}^1(\Omega))^3; \mathbf{v} = \mathbf{0} \text{ on } \Gamma\}, \tag{2}$$

where $\mathcal{H}^1$ denotes the corresponding Sobolev space, and the symmetric bilinear form $a(\mathbf{u}, \mathbf{v})$ and the linear form $f(\mathbf{v})$ are defined as:

$$a(\mathbf{u}, \mathbf{v}) = \int_\Omega \sum_{i,j=1}^{3} e_{ij}(\mathbf{u}) e_{ij}(\mathbf{v})\, dx, \tag{3}$$

$$f(\mathbf{v}) = \frac{1}{2\mu} \int_\Omega \mathbf{f} \cdot \mathbf{v}\, dx. \tag{4}$$

Here, $\mathbf{f} = (f_1, f_2, f_3)^t \in (L^2(\Omega))^3$ denotes the applied body forces,

$$e_{ij}(\mathbf{v}) = e_{ji}(\mathbf{v}) = \frac{1}{2}\left(\partial_j v_i + \partial_i v_j\right), \ \ i, j = 1, 2, 3 \tag{5}$$

is the linearized strain tensor, and μ is the Lamé elastic constant (which can also be considered as a scaling factor for the forces). The second elastic constant λ of the standard formulation was set to zero to eliminate one degree of freedom from the model. As a consequence, objects in images do not laterally shrink when being stretched. This makes sense in non-rigid registration (cf. [1]), since driving forces need only to be applied in the direction where the object is supposed to grow. The properties of the bilinear and linear form allow us to prove the existence and uniqueness of the solution of (2) (see [8], [14] for details).

A serious limitation of the linear model is the assumption of only small deformations, which is generally not true. To cope with large deformations, we introduce the second linearization of (1) which corresponds to our incremental model and is obtained by successively solving linear problems, starting from $\mathbf{u}^0 = \mathbf{0}$:

$$\mathbf{A}'(\mathbf{u}^{\mathrm{n}})\boldsymbol{\delta}\mathbf{u}^{\mathrm{n}} = \boldsymbol{\delta}\mathbf{f}^{\mathrm{n}}, \;\; n = 0, 1, \ldots \tag{6}$$

where $\boldsymbol{\delta}\mathbf{f}^{\mathrm{n}} = \mathbf{f}^{\mathrm{n}+1} - \mathbf{f}^{\mathrm{n}}$ and $\boldsymbol{\delta}\mathbf{u}^{\mathrm{n}} = \mathbf{u}^{\mathrm{n}+1} - \mathbf{u}^{\mathrm{n}}$. This formulation is also known as the Lagrangian incremental method [8].

The variational formulation of (6) with the parameter λ set to zero is given as [8]:

$$a(\boldsymbol{\delta}\mathbf{u}, \mathbf{v}) = l(\mathbf{v}), \quad \forall \mathbf{v} \in \mathbf{V}, \tag{7}$$

where

$$a(\boldsymbol{\delta}\mathbf{u}, \mathbf{v}) = \int_\Omega \sum_{i,j,p,q=1}^{3} \hat{a}_{ijpq}(\boldsymbol{\nabla}\mathbf{u}^n)\partial_p \delta u_q^n \partial_j v_i \, dx, \tag{8}$$

$$l(\mathbf{v}) = \frac{1}{\mu}\int_\Omega \boldsymbol{\delta}\mathbf{f}^n \cdot \mathbf{v} \, dx, \tag{9}$$

and

$$\hat{a}_{ijpq}(\nabla\mathbf{u}^n) = a_{ijpq} + \sum_{k=1}^{3} a_{kjpq}\partial_k u_i^n + \sum_{r=1}^{3} a_{ijrp}\partial_r u_q^n + \\ + \sum_{k,r=1}^{3} a_{kjpr}\partial_r u_q^n \partial_k u_i^n + \sum_{s,r=1}^{3} a_{pjsr}E_{sr}(\mathbf{u}^n)\delta_{iq}, \tag{10}$$

where $a_{ijpq} = \frac{1}{2}(\delta_{ip}\delta_{jq} + \delta_{iq}\delta_{jp}),\ i, j, p, q = 1, 2, 3$, δ_{ij} is Kronecker's symbol, and E_{sr} denotes the components of the Green-St. Venant strain tensor.

2.2 Parameter-Free Discrete Representation

We obtain discrete representations of both the linear and incremental model by using the *Galerkin method* [7], where the space $\mathbf{V}$ of admissible functions in the variational formulation is replaced by a finite-dimensional subspace $\mathbf{V}_N := \mathrm{span}\{\boldsymbol{\phi}_1, \boldsymbol{\phi}_2, \ldots, \boldsymbol{\phi}_N\}$. The solution vectors $\mathbf{u} = \{u_i\}$ of the linear model and $\boldsymbol{\delta}\mathbf{u} = \{\delta u_i\}$ of the incremental model are obtained from the resulting systems of linear equations.

We do not use any explicit external forces, and the elastic transformation is computed only due to the inhomogeneous boundary conditions. As a consequence, the remaining elastic parameter μ can be dropped together with the right-hand side of the model equations from the discrete formulations of (2) and (7), thus making our approach completely parameter-free.

The incorporation of prescribed displacements (or, respectively, displacement increments for the incremental model) has been realized through the conventional procedure to incorporate inhomogeneous boundary conditions into our FEM formulation (as described, for example, in [18]). According to this procedure, we have to modify the matrix of the linear system of equations by filling its rows and columns corresponding to the

nodal points where the displacements are prescribed with zero and setting the diagonal elements to one. The right-hand side vector of the modified system consists of the sum of the replaced matrix columns weighted by the prescribed values of displacements. It also contains these values in the positions corresponding to the nodal points where they were prescribed.

There is one important point which requires extra discussion. When applying the incremental method implemented on a discrete grid in the case of large deformations, the deformation gradient may locally approach zero after some iterations. As a consequence, the matrix of the discrete incremental formulation becomes badly conditioned and its further updates cannot be carried out.

To bypass this problem, we can use approximations of $\mathbf{A}'(\mathbf{u}^n)$ in the iteration process. One possible approximation can be obtained as

$$\mathbf{A}'(\mathbf{u}^n) \approx \mathbf{A}'(\mathbf{u}^k), \quad k = \max\{i \in \{0, \ldots, n\} \,|\, \det(\mathbf{I} + \boldsymbol{\nabla}\mathbf{u}^i) \geq \epsilon\}. \tag{11}$$

In other words, we do not compute the update of the stiffness matrix if the determinant of the deformation gradient locally falls below the threshold value ϵ. In this case, we preserve memory about a limited number of preceding deformations.

Another possibility is to take $\mathbf{A}'(\mathbf{u}^0) = \mathbf{A}'(\mathbf{0})$ as an approximation of $\mathbf{A}'(\mathbf{u}^n)$. This means that we do not carry memory about preceding deformations in our model. One advantage is that this method is computationally less expensive compared to the previous one.

3 Experimental Results

In this section, we present experimental results achieved with our registration approach.

In our first experiment, we registered a 3-D synthetic image with a part of cortical surface from a real image using the linear model. The computations took about 23 minutes on a R-8000 processor. We obtained prescribed displacements, needed as input data in our model, by matching the boundary of the cube with the cortical boundary using the 3-D minimal distance algorithm [2]. The size of both images was $80 \times 80 \times 80$ voxels. The result of the experiment is presented in the top row of Figure 1. Despite the complicated shape of the cortical surface, a rather good approximation of it has been obtained. In the middle row of Figure 1, magnitudes of the displacement field are shown for the slices 15, 30, 45. In the bottom row of the figure, the deformations of the slices 15, 30, 45 are represented as deformations of a rectangular regular grid.

In our next experiment, we registered 256×256 pre- and post-operative 2-D MR images of the same patient using the linear model. These images are depicted in the top row of Figure 2. The computations took about 80 seconds on a R-8000 processor. Prior to elastic registration, the two 3-D data sets were globally registered by using an affine transformation. For computation of this transformation, we used 5 pairs of landmarks which were manually localized. As corresponding structures for elastic transformation, we took the outer and the inner skin contours which were extracted by using an edge detector. Additionally, we used the brain surface contours, the contours of the right lateral ventricle, and the contour of the tumor in the source image together with the contour of the resection area in the target image which were manually as well as semi-automatically (using a snake approach [13]) determined. They are depicted in the middle row of Figure 2. We

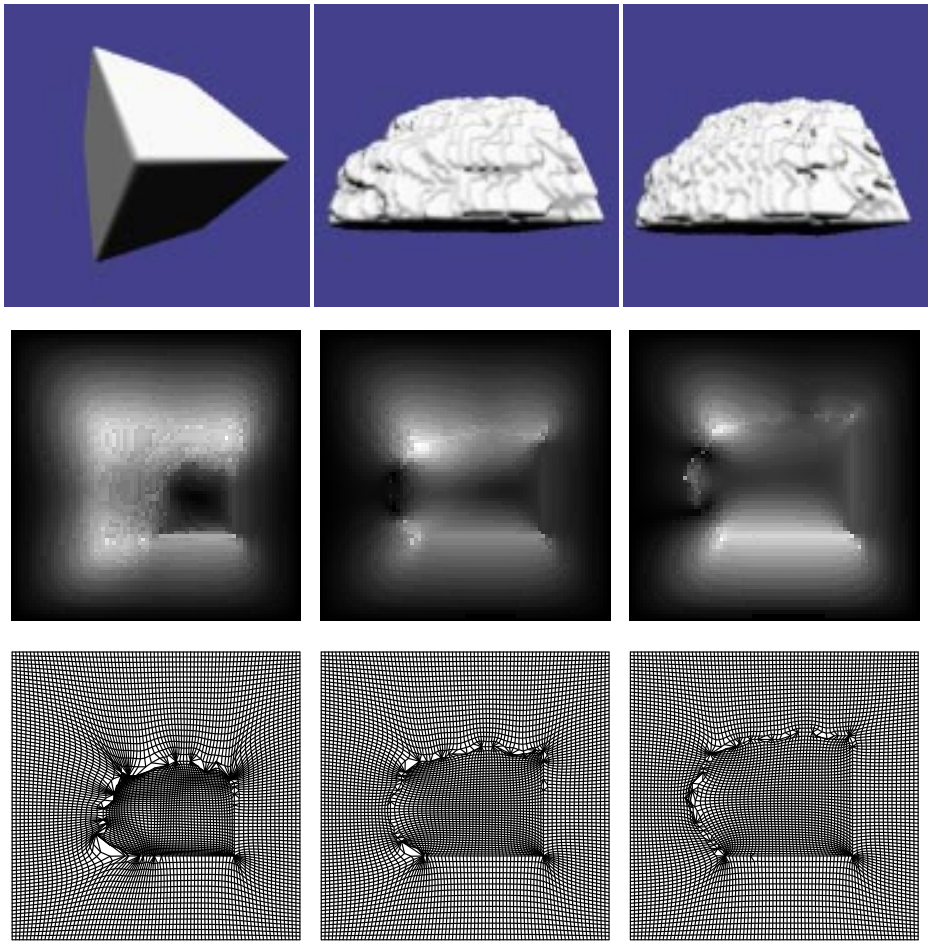

Figure 1: 3-D registration experiment. Top row: Source, target, and deformed source images. Middle row: Magnitudes of the displacement field for the horizontal slices 15, 30, 45. Bottom row: Deformations of the horizontal slices 15, 30, 45 projected onto the *xy*-plane and illustrated by a grid.

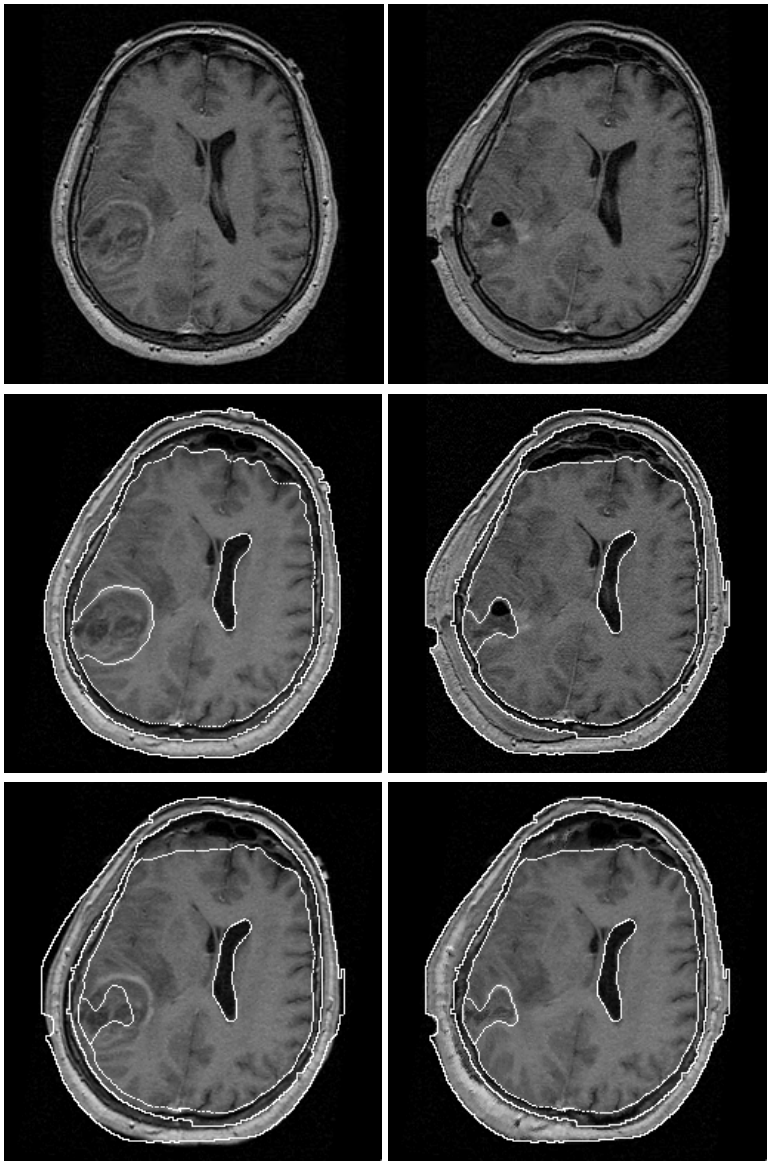

Figure 2: 2-D registration example. Top row: Two MR slices taken from the same patient with the pre-operative source image at the left. Middle row: Corresponding structures in the globally transformed source image and in the target image. The pre- and post-operative tumor outlines have been kindly provided by OA Dr. med. U. Spetzger of the Neurosurgical Clinic, Aachen University of Technology (RWTH). Bottom row: Registration results. Left image: Result of affine registration. Right image: Result of elastic registration.

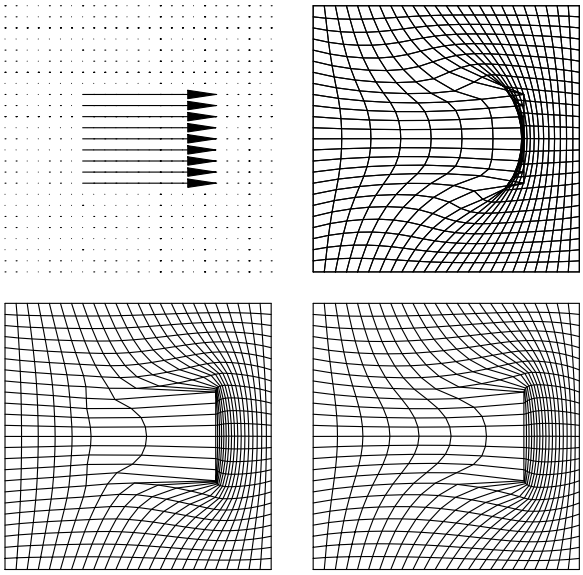

Figure 3: Comparison between the linear and incremental registration model. Top row/left: Prescribed displacements. Top row/right: Computed deformation using the linear model. Bottom row: Computed deformation using the incremental model with memory (left) and without memory (right). One can see that the incremental model preserves the grid topology when computing large deformations.

also fixed two boundary structures in the source image: the occipital part of the midline of the brain and a part of the *dura mater* in the brain shift area at the top of the brain. The input data for elastic transformation were obtained through the use of the minimal distance algorithm (for the skin contours) and from the snake model for all other structures (see [15] for more details about obtaining correspondences using the snake model). The result of elastic registration is shown in the right image of the bottom row of Figure 2. One can see that a more accurate match of the corresponding anatomical structures has been achieved after elastic registration compared to global affine registration (left image). Local elastic transformation has also allowed to cope with metamorphic processes due to the tumor resection. For a different approach to cope with deformations due to brain shifts which is based on a three component tissue model, see also [11].

Our linear model may cause topology violations in the deformed image in the case of large deformations. For illustration purposes, a comparison between the linear model and incremental model with and without memory in the case of a large deformation is presented in Figure 3. The value of ϵ in (11) for this experiment was chosen to be 0.2. One can see that both incremental models preserve grid topology in contrast to the linear model. However, the deformation computed with the model without memory is more smooth. The choice between the two incremental models should be made in dependence of a concrete application.

4 Conclusion

In this paper, we have described a parameter-free elastic registration approach where images are elastically deformed through incorporation of prescribed displacements obtained by mapping boundary structures. We have presented experimental results for a linear and an incremental model, where the latter model generally allows to cope with large deformations, as it has been demonstrated for a synthetic example.

Since our approach does not contain any parameters of the deformation model, only the input data can influence the registration result. Hence accuracy of the input data plays a crucial role for the success of our registration approach. From experimental results, we can conclude that good registration results can be obtained if correct input data are available. Very complex shapes of objects in medical images make the development of methods which allow to precisely determine the point mapping between boundary structures a very challenging task. As examples of such techniques, we have used the minimal distance algorithm and a snake model. However, their practical usage, for example in the case of irregular contour shapes, is limited. The development of more reliable methods is the objective of current research.

Another important point of future research is the efficient numerical implementation of our approach. The implemented method of conjugate gradients with preconditioning shows acceptable results if the matrix can completely be loaded into the computer memory (several seconds in 2-D and minutes in 3-D). However, it is not always possible in the 3-D case due to the large number of variables of the deformation model. Hence prior to the usage of our approach in real medical applications, further developments, e.g. explicit parallelization and possibly multi-grid techniques, are required.

Acknowledgments

Medical image data were kindly provided by Philips Research Laboratories Hamburg and OA Dr. med. U. Spetzger of the Neurosurgical Clinic, Aachen University of Technology (RWTH).

References

[1] R. Bajcsy and S. Kovačič. Multiresolution elastic matching. *Computer Vision, Graphics, and Image Processing*, 46:1–21, 1989.

[2] P.J. Besl and N.D. McKay. A method for registration of 3-D shapes. *IEEE Transactions on Pattern Analysis and Machine Intelligence*, 14(2):239–256, 1992.

[3] F.L. Bookstein. Principal warps: Thin-plate splines and the decomposition of deformations. *IEEE Transactions on Pattern Analysis and Machine Intelligence*, 11(6):567–585, 1989.

[4] M. Bro-Nielsen and C. Gramkow. Fast fluid registration of medical images. In *Proc. Visualization in Biomedical Computing (VBC'96)*, pages 267–276, Hamburg, Germany, September 1996. Springer-Verlag.

[5] C. Broit. *Optimal Registration of Deformed Images*. Doctoral dissertation, University of Pennsylvania, August 1981.

[6] G.E. Christensen, R.D. Rabbitt, and M.I. Miller. Deformable templates using large deformation kinematics. *IEEE Transactions on Image Processing*, 5(10):1435–1447, 1996.

[7] P.G. Ciarlet. *The Finite Element Method for Elliptic Problems*. North-Holland, Amsterdam, 1978.

[8] P.G. Ciarlet. *Mathematical Elasticity. Volume I: Three-Dimensional Elasticity*. North-Holland, Amsterdam, 1988.

[9] C. Davatzikos. Spatial transformation and registration of brain images using elastically deformable models. *Computer Vision and Image Understanding, Special Issue on Medical Imaging*, 66(2):207–222, 1997.

[10] C. Davatzikos, J.L. Prince, and R.N. Bryan. Image registration based on boundary mapping. *IEEE Transactions on Medical Imaging*, 15(1):112–115, 1996.

[11] P.J. Edwards, D.L.G. Hill, J.A. Little, and Hawkes. D.J. Deformation for image guided interventions using a three component tissue model. In J. Duncan and G. Gindi, editors, *Proc. 15th Internat. Conf. Information Processing in Medical Imaging (IPMI'97)*, pages 218–231, Poultney, Vermont, USA, June 1997. Springer-Verlag.

[12] J.C. Gee, D.R. Haynor, M. Reivich, and R. Bajcsy. Finite element approach to warping brain images. In *Proc. SPIE Image Processing*, volume 2167, pages 327–337, 1994.

[13] M. Kass, A. Witkin, and D. Terzopoulos. Snakes: Active contour models. *International Journal of Computer Vision*, 1(4):321–331, 1988.

[14] W. Peckar. FEM dicretization of the Navier equation with applications to medical imaging. Memo FBI-HH-M-266/96, Dept. of Computer Science, University of Hamburg, November 1996.

[15] W. Peckar, C. Schnörr, K. Rohr, and H.S. Stiehl. Two-step parameter-free elastic image registration with prescribed point displacements. In *Proc. 9th Int. Conf. on Image Analysis and Processing (ICIAP '97)*, pages 527–534, Florence, Italy, September 1997. Springer-Verlag.

[16] K. Rohr, H.S. Stiehl, R. Sprengel, W. Beil, T.M. Buzug, J. Weese, and M.H. Kuhn. Point-based elastic registration of medical image data using approximating thin-plate splines. In *Proc. Visualization in Biomedical Computing (VBC'96)*, pages 297–306, Hamburg, Germany, September 1996. Springer-Verlag.

[17] T. Schormann, S. Henn, and K. Zilles. A new approach to fast elastic alignment with applications to human brains. In *Proc. Visualization in Biomedical Computing (VBC'96)*, pages 337–342, Hamburg, Germany, September 1996. Springer-Verlag.

[18] H.R. Schwarz. *Methode der finiten Elemente*. Teubner, Stuttgart, 1984.